Available online at www.sciencedirect.com
SCIENCE DIRECT
Applied Surface Science 252 (2006) 4599–4603
applied surface science
www.elsevier.com/locate/apsusc

Structural characterization and magnetoresistance of manganates thin films and Fe-doped manganates thin films

S. Canulescu [a], Th. Lippert [a,*], H. Grimmer [a], A. Wokaun [a], R. Robert [b], D. Logvinovich [b], A. Weidenkaff [b], M. Doebeli [c]

[a] *Paul Scherrer Institut, CH-5232 Villigen, Switzerland*
[b] *EMPA, CH-8600 Duebendorf, Switzerland*
[c] *Paul Scherrer Institut c/o ETH Zürich, CH-8093 Zurich, Switzerland*

Received 3 May 2005; accepted 15 July 2005
Available online 2 November 2005

Abstract

Perovskites thin films with the composition $La_{0.6}Ca_{0.4}MnO_3$ doped with 20% Fe, were prepared by pulsed reactive crossed beam laser ablation, where a synchronized reaction gas pulse interacts with the ablation plume. The films were grown on various substrates and the highest colossal magnetoresistance ratio (CMR) was detected by Hall measurements for films grown on $LaAlO_3$ (1 0 0), which was selected as substrate for further investigations.

Several growth parameters, such as substrate temperature and target to substrate distance were varied to analyze their influence on the film properties.

The structure of the deposited thin films was characterized by X-ray diffraction and atomic force microscope, while Rutherford backscattering (RBS) was used to determine the film stoichiometry. The electrical properties were determined by Hall effect measurements in a magnetic field of 0.51 T.

These measurements reveal that the amplitude of the CMR ratio depends strongly on the substrate and that the oxygen content influences the temperature where the transition from semiconductor to metal is observed.

Keywords: Magnetoresistance; Manganates thin films; Fe-doped manganates thin films; Pulsed laser deposition

1. Introduction

Recent investigations on perovskite-type compounds such as $La_{1-x}A_xMnO_3$ (A = Ca, Sr, Ba) have shown a spectacular increase of the resistivity by several orders of magnitude in the presence of a magnetic field. This effect has been named colossal magnetoresistance [CMR = $\rho(H) - \rho(0)/\rho(0)$], in contrast to giant magnetoresistance, which refers to an increase/decrease of the resistivity up to 20% in presence of magnetic fields.

Even larger magnetoresistance values have been reported for thin films compared to the bulk materials [1]. An increase by 90% of the magnetoresistance was observed in $Nd_{0.67}Sr_{0.33}MnO_3$ epitaxial thin films [2], which leads to the conclusion that thin films could be suitable candidates for future applications such as magnetic sensors or magnetoresistive reading heads for information storage systems [3]. The properties which need to be improved for these compounds, especially in manganates materials, are the small values of the magnetoresistance at room temperature and in weak magnetic fields [4].

The film microstructure and the strain induced in the film or/and at the substrate–film interface due to the lattice mismatch between the film and the substrate are very important factors that affect the magnetic, ferroelectric [5] and transport properties of thin films [6,7]. It has been reported that the lattice mismatch between the film and the substrate influences the transition temperature from metallic to semiconducting of $La_{1-x}Ca_xMnO_3$ compounds [4,8]. The applied substrates can induce different strain-type in the films, e.g. tensile or compressive stress, resulting in films that exhibit different transport properties that vary from metallic to insulating [9]. Detailed investigations on

* Corresponding author. Tel.: +41 563104076; fax: +41 563102688x2199.
E-mail address: Thomas.Lippert@psi.ch (T. Lippert).

0169-4332/$ – see front matter © 2005 Elsevier B.V. All rights reserved.
doi:10.1016/j.apsusc.2005.07.151

$La_{1-x}Ca_xMnO_3$ ($x = 0.33$, 0.5) thin films showed that tensile strain induces an increase of the resistivity and magnetoresistance, while compressive strain has the opposite effect [4].

One mechanism that is used to explain the CMR behavior of these materials is the double-exchange (DE) interaction [10]. Doping the insulating $LaMnO_3$ with 20–50% Ca on the A-site, creates mixed valences of Mn^{3+}/Mn^{4+}. In the Mn^{3+}–O–Mn^{4+} network, the e_g electrons are hopping from the Mn^{3+} ions to the Mn^{4+} ions via the DE interaction which induce metallic conductivity in manganates [11]. Any deviation of the Mn–O–Mn bond length or bond angle affects the DE mechanism. The Mn^{3+} ions are mainly responsible for the DE mechanism and a partial replacement of the Mn^{3+} with other transition metals, e.g. Fe, Ni will therefore influence the DE mechanism [12].

We report the growth of $La_{0.6}Ca_{0.4}MnO_3$ (LCMO) and Fe-doped LCMO thin films on $LaAlO_3$ (1 0 0), $SrTiO_3$ (1 0 0) and MgO (1 0 0) substrates. Higher substrate temperatures, e.g. in the range of 600 to 750 °C, have been reported to favor a higher quality of the epitaxial films and an increase of the MR ratio [13]. A variation of pulsed laser deposition, i.e. pulsed reactive crossed beam laser ablation (PRCLA) [14], has been applied to minimize and control the oxygen deficiency in the films [15].

2. Experiment

A KrF ($\lambda = 248$ nm, $\nu = 10$ Hz) excimer laser was used at a laser fluence of 7 J/cm^2. The $La_{0.6}Ca_{0.4}MnO_3$ (LCMO) and $La_{0.6}Ca_{0.4}Mn_{0.8}Fe_{0.2}O_3$ (LCMFO) thin films with thicknesses ranging from 100 to 330 nm were prepared by PRCLA. Details of the method have been described elsewhere [15]. Briefly, the laser-induced plasma beam crosses the molecule beam (N_2O and O_2) from the gas pulse, which has a length of 400 μs. A low O_2 background pressure was maintained in the chamber (8×10^{-2} Pa) during the deposition process. The substrates were heated to 600 and 650 °C with an average heating rate of 8 °C/min. Single crystalline $LaAlO_3$ (1 0 0), $SrTiO_3$ (1 0 0) and MgO (1 0 0) substrates, with a cubic crystal structure were used for the deposition process.

The surface morphology of the films was analyzed using an atomic force microscope (AFM) from Park Instruments while the films thickness was measured with a profilometer (Dektak 8000). The AFM measurements were performed in contact mode and the roughness values were obtained from 20 μm × 20 μm and 5 μm × 5 μm scan areas.

X-ray diffraction (XRD) patterns were recorded using a SEIFFERT 3000P diffractometer, using standard θ:2θ scans. For some samples a Siemens (D5000) diffractometer was applied, equipped with an Eulerian cradle for texture analysis.

The samples compositions of the films were determined by Rutherford backscattering (RBS) spectrometry and elastic recoil detection analysis (ERDA). The RBS measurements were performed using a 2 MeV ^{4}He beam and a silicon surface barrier detector at 165°. The collected RBS data were simulated using the RUMP software [16]. For the ERDA analysis a 12 MeV ^{127}I beam was used under incidence angle of 18°. The scattered recoils were identified by the combination of a time-of-flight spectrometer with a gas ionization chamber.

The resistivity versus temperature curves [$\rho = \rho(T)$] were measured by the four-point method, using a Hall effect measurement system (EGK-Holdings) and from room temperature to liquid nitrogen temperature. The magnetoresistance was measured by applying a magnetic field of 0.51 T.

3. Results and discussions

3.1. Atomic force microscopy

The roughness (RMS values) for all films was measured for a scan area of 5 μm × 5 μm and is in the range of 1–7 nm. The 2D scans of $La_{0.6}Ca_{0.4}Fe_{0.2}Mn_{0.8}O_3$ films, i.e. on $LaAlO_3$ and $SrTiO_3$ (shown in Fig. 1) reveal an island-like growth, which is related to the epitaxial crystal structure of the thin films [17]. Uniformly distributed round shaped grains of equal sizes are observed for both substrates. An analysis on the roughness parameters (RMS) is listed in Table 1.

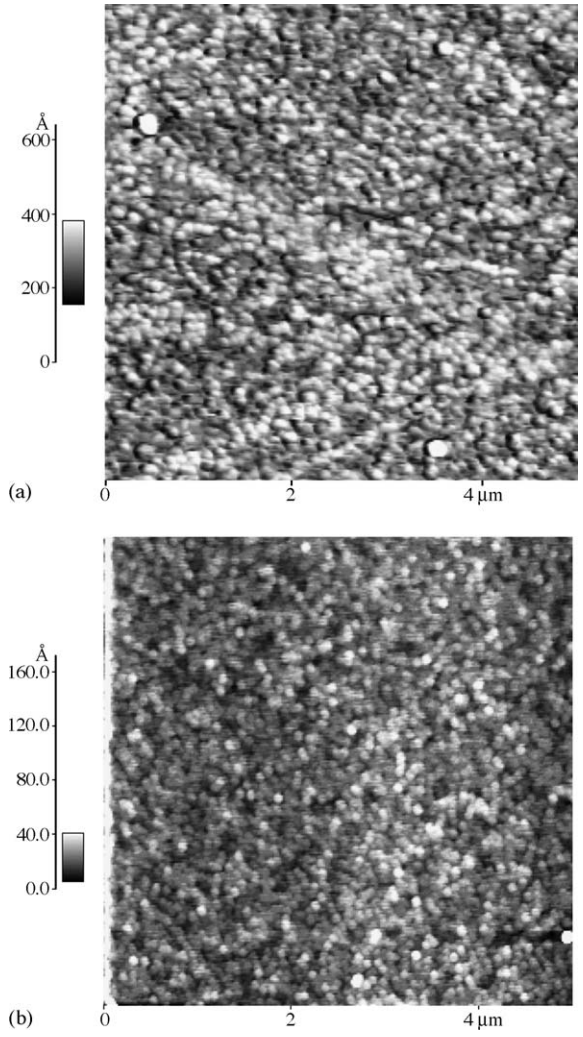

Fig. 1. AFM images of the Fe-doped films grown on (a) LAO and (b) STO at a substrate temperature of 600 °C and a target–substrate distance of $D_{T-S} = 3.5$ cm.

Table 1
Film topography and thickness of LCMO and LCMFO

Film	Thickness (nm)	Average grain size (nm)	RMS (nm)[a]
Fe-doped LCMO on $SrTiO_3$	130	120	4.8
Fe-doped LCMO on $LaAlO_3$	120	45	1.7
LCMO on $LaAlO_3$	330	160	6.9

[a] RMS: root mean square roughness.

In general, an increase of the grain size and surface roughness is observed for an increase of the target–substrate distance in the range from 3.5 to 5 cm. For target to substrate distances of 3.5 cm an average grain size of 58 nm and RMS = 17.5 nm value was measured, while for 5 cm an average grain size of 65 nm and RMS = 4.3 nm. Similar surface morphology observed at 3.5 and 4 cm is probably due to the position of the substrate within the plume, which increases in size due to the collisions between the plasma and the gas pulse molecules [18]. The influence of the temperature on the film topography was probed at two temperatures, e.g. 600 and 650 °C, for LCMO films on LAO. The substrate temperature has a pronounced influence on the nucleation mode of the films, which can result in different film topographies.

In the case of LCMO films, a substrate temperature of 650 °C induces an island-like growth with a homogeneous distribution of the islands. At lower temperatures the nucleation phase occurs faster and a lower coverage by islands is observed (see Fig. 2). This difference can be explained by the higher mobility of the species on the substrate surface at the higher temperature.

3.2. X-ray diffraction and films composition

The XRD patterns of the LCMO films and Fe-doped LCMO films are shown in Fig. 3. The crystallographic structure of the films is pseudocubic and belongs to the space group $Pm\bar{3}m$. The lattice parameters of the films, corresponding to the pseudocubic unit cell that is described by the relations $a_p = a = b = c$ and $\alpha = \beta = \gamma \sim 90°$, give a value $a_p \approx 0.39$ nm.

The films deposited on LAO and STO substrates show an epitaxial relationship with the substrate, while the films grown on MgO substrates are polycrystalline (not shown here). The lattice parameters of the LAO, STO, MgO substrates with cubic structure are $a = 0.379078, 0.39012$ and 0.421 nm, respectively. The lattice mismatch α along the interface, defined as $\alpha = (a_{psubstrate} - a_{pbulk})/a_{psubstrate}$, gives the following values for the substrates used: $\alpha_{LAO} \approx -0.028\%$, $\alpha_{STO} \approx 0.0003\%$ and $\alpha_{MgO} \approx 0.07\%$. Tensile strain appears at the film–substrate interface in the case of STO and MgO substrates while for LAO substrates, a compressive strain results. The substrate-type used in the deposition process has a major influence in the film microstructure and the low lattice mismatch between the film and substrate results in an epitaxial growth of the LCMO thin films on LAO and STO. It was observed that higher substrate temperatures during the deposition yield a better epitaxial relationship. Full-width at half maximum (FHWM) of the

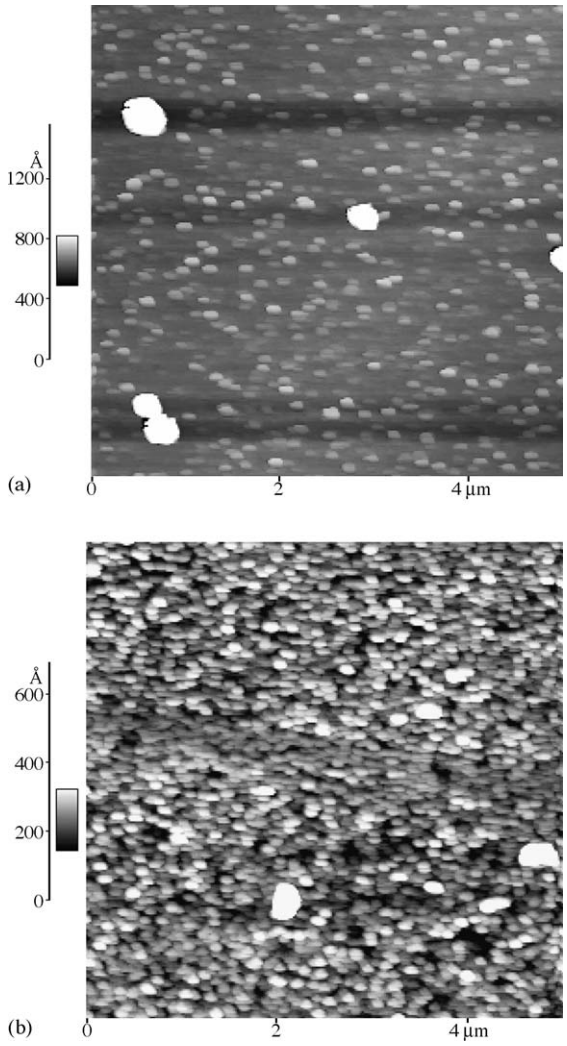

Fig. 2. (2D) view of the LCMO films deposited on LAO substrate at 600 °C (a) and 650 °C (b). Both films have a thickness of around 330 nm.

(2 0 0) peak for the Fe-doped LCMO films (thickness = 100 nm) was 0.397 for $T_s = 600$ °C and 0.2095 for $T_s = 650$ °C. Also, in the case of MgO substrate, the lattice mismatch value is not significant but the deposition performed

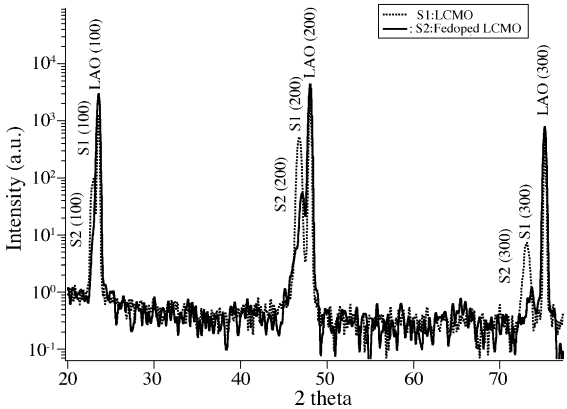

Fig. 3. XRD pattern of the LCMO thin films and Fe-doped LCMO thin films grown on LAO (1 0 0) substrates.

Table 2

Nominal composition of the targets[a]	Films compositions (La/Ca/Mn/Fe/O)
$La_{0.6}Ca_{0.4}Fe_{0.2}Mn_{0.8}O_3$	$La_{0.72\pm0.036}$ $Ca_{0.28\pm0.014}Fe_{0.2\pm0.05}Mn_{0.8\pm0.05}O_{2.5\pm0.125}/SrTiO_3$
$La_{0.6}Ca_{0.4}MnO_3$	$La_{0.72\pm0.036}Ca_{0.28\pm0.014}Mn_{0.85\pm0.0425}O_{2.4\pm0.12}/LaAlO_3$
$La_{0.6}Ca_{0.4}Fe_{0.2}Mn_{0.8}O_3$	$La_{0.66\pm0.033}Ca_{0.34\pm0.017}Fe_{0.2\pm0.05}Mn_{0.8\pm0.05}O_{2.6\pm0.13}/LaAlO_3$

[a] Given by the manufactory (Proxair).

at 650 °C substrate temperature was not sufficient for an epitaxial growth. Further investigations will be carried out for optimization of the growth conditions.

A substitution of 20% of Mn by Fe results in a minor change of the crystal structure and a shift of the main reflex by 0.35°.

The film composition, obtained from RBS measurements reveals that the films exhibit pronounced oxygen deficiencies (see Table 2). The precision of the quantitative film composition (atomic ratio) is in the range from 5 to 9%. It was impossible to distinguish Mn from Fe by RBS measurements due to the small difference in the atomic weight of the elements, which is around 0.91 amu. It was also not possible to determine the Mn/Fe ratio by ERDA measurements. Therefore, the nominal Mn/Fe ratio was used to obtain the ratio of the other elements.

In order to decrease the oxygen deficiency in the films, further experiments will be performed with N_2O as a gas pulse. Recent investigations have shown that by applying N_2O as a background gas during the PLD experiments, an increase of the oxidation of Mn in the plasma plume occurs. The resulting films, i.e. $La_{0.67}Sr_{0.33}MnO_3$ show an improvement of the magnetic properties [19]. It was also observed that a higher oxygen content and good crystallographic quality were obtained by using the N_2O as a gas pulse on $La_{0.6}Ca_{0.4}CoO_3$ thin films grown by PRCLA [20].

3.3. Electrical transport properties of the LCMO and LCMFO thin films

The dependence of the resistivity as a function of the temperature for LCMO thin films on LAO and STO with the same thickness (195 nm) is shown in Fig. 4. Both films exhibit a similar behavior, i.e. a transition from the semiconductor state to the metallic (T_{IM}) state. For the films deposited on LAO substrates a shift of the transition temperature by +46 K was observed, compared to the film grown on STO. The same tendency, i.e. a shifting of the T_{IM} to higher temperature was observed on $La_{0.7}Ca_{0.3}MnO_3$ films for STO and LAO as substrates [8].

The thin films show a maximum magnetoresistance value at the temperature corresponding to the metal–insulator transition, i.e. 20% MR at the T_{IM} = 109 K for LAO (shown in Fig. 5). The films grown on LAO have the lowest lattice mismatch and exhibit a tensile strain while for MgO and STO compressive strain is expected. It has been suggested that compressive strain results in a compression of the Mn–O bond length [21], which allows an easier transfer of the e_g electrons between the Mn^{3+} and Mn^{4+} ions. Thus a slight

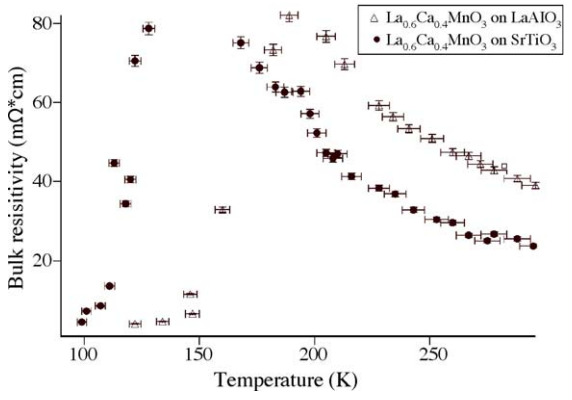

Fig. 4. Temperature dependence of the resistivity measured for the LCMO films grown on $SrTiO_3$ and $LaAlO_3$ substrates. The thickness of both films is 194 nm.

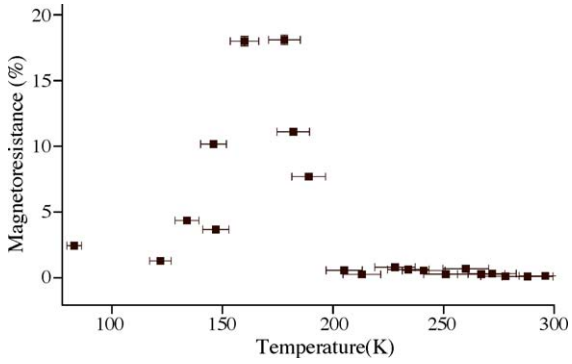

Fig. 5. The magnetoresistance $\Delta\rho/\rho_0$ of the LCMO thin films grown on $LaAlO_3$. Film thickness is 194 nm.

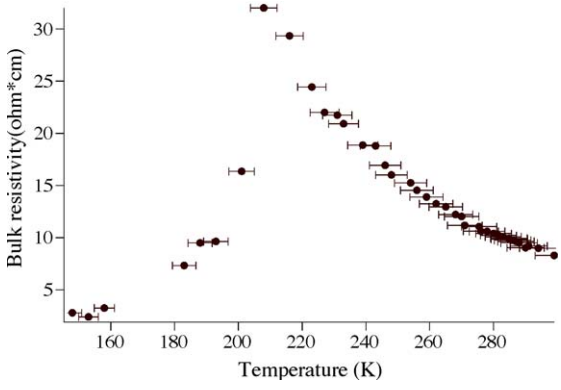

Fig. 6. Resistivity vs. temperature dependence of the LCMFO films deposited on $LaAlO_3$ substrates.

decrease of the resistivity is observed for LAO compared with STO.

A 20% substitution of Mn by Fe results in an increase of the resistivity value from 5 to 30 Ω cm and the transition T_{IM} occurs at a temperature of 208 K which is 19 K higher than for the LCMO films on LAO (see Fig. 6). As the Mn is substituted by Fe ($x = 0.2$), a magnetoresistance (MR) value less than 1% was measured at magnetic field of 0.51 T. As we mentioned above, the double-exchange mechanism is decisive for the magnetoresistive effect. The Mn^{3+} ions are replaced in the LCMFO films by the Fe ions which do not participate in the double-exchange interaction and therefore suppress the conduction of the e_g electrons in the network Mn^{3+}–O_2–Mn^{4+}. A shift of the T_{IM} temperature to higher temperatures is therefore observed, which is a desired direction for industrial applications. More investigations will be carried out on Fe-doped LCMO thin films at higher magnetic fields in order to confirm the CMR effect.

4. Conclusions

High quality $La_{0.6}Ca_{0.4}Mn_{1-x}Fe_xO_3$ ($x = 0$, 0.2) epitaxial thin films have been grown on $LaAlO_3$ and $SrTiO_3$ substrates. At higher substrate temperature ($T_s \approx 650$ °C) films with high epitaxial quality and island-like growth with low surface roughness values (RMS 10–50 Å) are observed. The films deposited on $LaAlO_3$ substrates have the lowest film to substrate lattice mismatch and exhibit the best magnetoresistive properties. The substitution of Mn ions by Fe ions in the crystal structure results in a shift of the metal–semiconductor temperature and lead to a suppression of the CMR effect, the magnitude of the CMR ratio being less than 1%.

Acknowledgments

The authors thank the Paul Scherrer Institut for financial support and to Dr. Flavio Campana for helpful advices in the AFM measurements.

References

[1] Y. Ueda, T. Nakajim, J. Phys.: Condens. Matter 16 (2004) S573.
[2] C. Kong, Y.L. Chang, Appl. Phys. A: Mater. Sci. Process. A 70 (2004) 2103.
[3] Ph. Lecoeur, B. Merce, W. Prellier, J. Phys.: Condens. Matter. 13 (1993) R915.
[4] Y.M. Xiong, G.Y. Wang, X.G. Luo, J. Appl. Phys. 97 (8) (2005) 083909.
[5] J.H. Haeni, P. Irvin, W. Chang, Nature 430 (2004) 758.
[6] E. Gommert, H. Cerva, J. Wecker, K. Samwer, J. Appl. Phys. 85 (1999) 5417.
[7] M.J. Casanove, C. Roucau, P. Baules, Appl. Surf. Sci. 188 (2002) 19.
[8] Z.L. Wang, C.J. Lu, C. Kwon, Q.X. Jia, J. Appl. Phys. 88 (2000) 4032.
[9] Z.F.Y. Konishi, M. Izumi, T. Manako, M. Kasai, H. Kuwahara, M. Kawasaki, K. Terakura, Y. Tokura, J. Phys. Soc. Jpn. 68 (1999) 3790.
[10] C. Zener, Phys. Rev. 82 (1951) 403.
[11] A.-M. Haghiri-Gosnet, J.-P. Renard, J. Phys. D: Appl. Phys. 36 (2003) R127.
[12] C.J. Liu, L.S. Hsu, T.W. Wu, D. Luca, J. Opt. Adv. Mater. 5 (2003) 409.
[13] Y.S. Leung, K.H. Wong, Appl. Surf. Sci. 491 (1998) 127.
[14] P.R. Willmott, Appl. Phys. A: Mater. Sci. Proces. 69 (7) (1999) S437.
[15] M.J. Montenegro, C. Clerc, T. Lippert, Montenegro, Muller, S. Willmott, A. Weidenkaff, A. Wokaun, Appl. Surf. Sci. 45 (2003) 208.
[16] L.R. Doolittle, Nucl. Instr. Meth. B15 (1986) 227.
[17] G.K. Chrisey, Hubler, Pulsed Laser Deposition of thin films, John Wiley & Sons Inc., 1994,, p. 260.
[18] P.R. Willmott, Appl. Phys. A 69 (1999) S437.
[19] A. Gupta, P. Lecoeur, P.R. Duncombe, G.Q. Gong, G. Xiao, J. Appl. Phys. 80 (1996) 513.
[20] M. Dobeli, M.J. Montenegro, T. Lippert, S. Muller, A. Weidenkaff, P.R. Willmott, A. Wokaun, Thin Solid Films 453–454 (2004) 182.
[21] M. Marezio, P.G. Radaelli, G. Iannone, H.Y. Hwang, S.-W. Cheong, J.D. Jorgensen, D.N. Argyriou, Phys. Rev. B 56 (1997) 8265.